ACS Macro Letters
Letter
pubs.acs.org/macroletters

Random Poly(3-hexylthiophene-*co*-3-cyanothiophene) Copolymers via Direct Arylation Polymerization (DArP) for Organic Solar Cells with High Open-Circuit Voltage

Andrey E. Rudenko, Petr P. Khlyabich, and Barry C. Thompson*

Department of Chemistry and Loker Hydrocarbon Research Institute, University of Southern California, Los Angeles, California 90089-1661, United States

Supporting Information

ABSTRACT: A family of four poly(3-hexylthiophene) (P3HT) based copolymers containing 5, 10, 15, and 20% of 3-cyanothiophene (CNT) incorporated in a random fashion with a regioregular linkage pattern (P3HT-CNT) were successfully synthesized via direct arylation polymerization (DArP). Unique reaction conditions, previously reported for P3HT, were used, which employ very low loadings of $Pd(OAc)_2$ as a catalyst and an inexpensive bulky carboxylic acid (neodecanoic acid) as an essential part of the palladium catalytic center. The chemical structures and optoelectronic properties of DArP P3HT-CNT polymers were found to be similar to those of previously investigated P3HT-CNT polymers synthesized via Stille polycondensation. All polymers are semicrystalline with high hole mobilities and UV−vis absorption profiles that resemble P3HT, while the polymer highest occupied molecular orbital (HOMO) level decreases with increasing content of cyanothiophene in both DArP and Stille P3HT-CNT polymers. In photovoltaic devices with a $PC_{61}BM$ acceptor, DArP P3HT-CNT copolymers showed slightly lower open-circuit voltages (V_{oc}) than their Stille P3HT-CNT analogues but similar fill factors (FF) and significantly enhanced short-circuit current densities (J_{sc}), leading to overall power conversion efficiencies for the DArP polymers that rivaled or exceeded those of the Stille polymers. This work further emphasizes the generality and relevance of DArP for the synthesis of conjugated polymers for use in organic solar cells and the attractive simplicity and ease of synthesis of random conjugated polymers.

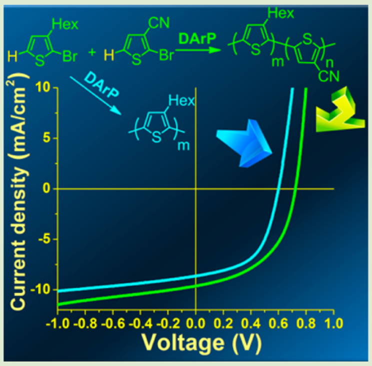

Direct arylation polymerization (DArP)[1−5] has emerged in the last several years as an attractive alternative to traditional methods of transition-metal-catalyzed cross-coupling polymerizations for the synthesis of conjugated polymers, such as Stille,[6] Suzuki,[7] Kumada,[8] Negishi,[9] and, most recently, Murahashi[10] polymerizations. Unlike all these methods that require a metalated aromatic ring as one functionality and a halogenated (usually, brominated) aromatic ring as another functionality, DArP allows polymerization of unmetalated monomers containing a C_{Ar}−H bond and C_{Ar}−Br bond, leading to high molecular weight conjugated polymers with high yield. The elimination of the metalation step makes DArP an attractive synthetic route since very often the metalation itself and purification of the metalated monomers can be challenging[11] due to their instability as well as the toxicity[12] associated with, for example, the frequently used Stille polymerization.

Conjugated polymers prepared by DArP have been targeted for various applications including organic photovoltaics (OPV).[13−18] As a technology, which is viewed as a simple and environmentally friendly energy conversion platform, OPV is certain to benefit from material synthesis simplification and elimination of toxic waste offered by DArP.[19] Despite numerous reports on using DArP for the synthesis of both wide band gap and low band gap polymers the reports of their OPV performance are less common. At the same time, it is very important to establish the suitability of this new polymerization method for photovoltaic applications since in the past certain methods of conjugated polymer synthesis (electropolymerization,[20] chemical oxidative polymerization)[21] were indeed found to not be suitable for OPV.[22] Recently, Heeger et al. reported thienopyrrolodione-containing wide band gap copolymers with power conversion efficiency (PCE) exceeding 6%;[13,14] Tacca et al. reached 1.48% PCE with a benzodithiophene-based intermediate band gap copolymer;[17] and Horie et al. achieved 3.98% PCE with low band gap poly[2,6-(4,4-bis(2-ethylhexyl)-4*H*-cyclopenta[2,1-*b*;3,4-*b*′]dithiophene)-*alt*-4,7(2,1,3-benzothiadiazole)] (PCPDTBT) synthesized by DArP.[18] However, the common feature of all these polymers, and state-of-the-art polymers in general, is complex multistep synthesis of monomers. As a result, easily synthesized polymers, with minimal number of synthetic steps that yield high open-circuit voltage (V_{oc}) and short-circuit current density (J_{sc}) in OPV, are in great demand, and the photovoltaic properties of such polymers synthesized via DArP have not been reported.

Recently, we have reported a family of four novel poly(3-hexylthiophene) (P3HT) analogues containing 5−20% of a simple electron-deficient 3-cyanothiophene (CNT) unit

Received: March 19, 2014
Accepted: April 1, 2014
Published: April 3, 2014

incorporated into the polymer backbone in the random fashion with regioregular linkage pattern via Stille polycondensation for photovoltaic application.[23] Similarly to what has been established earlier for the case of 3-(2-ethylhexyl)thiophene,[24] the randomized incorporation of a small amount of 3-cyanothiophene in the polymer backbone preserved semicrystalline nature inherent for regioregular P3HT while exhibiting lower-lying highest occupied molecular orbital (HOMO) levels, which results in solar cells with high FFs and high J_{sc} similar to P3HT:PC$_{61}$BM, but with an increased V_{oc}.[23] As illustrated in Scheme 1, this family of P3HT-CNT copolymers was synthesized via Stille polymerization using 2-bromo-3-hexyl-5-trimethylstannylthiophene (**3**) and 2-bromo-3-cyano-5-trimethylstannylthiophene (**4**). The synthesis of the latter monomer **4** was found to be very challenging to perform using the traditional method of lithiation−stannylation presumably due to the instability of the lithiated species toward the halogen dance reaction and immediate isomerization even at −78 °C. This problem has been solved by using the Knöchel−Hauser base[25] instead of LDA and generating less reactive and more stable magnesiated species with subsequent quenching with trimethyltin chloride to yield the target stannylated monomer. This synthetic approach allows preparation of regioregular random P3HT-CNT with a greater variety of unit linkages than in the previously reported perfectly alternating copolymers containing alkylthiophene and CNT.[26] At the same time, it also illustrates the challenges that may arise on the metalation step, suggesting that the P3HT-CNT family will become even more attractive if the monomer metalation step is eliminated.

Scheme 1. Synthetic Scheme for the Synthesis of P3HT-CNT: (a) via DArP and (b) via Stille Polymerization

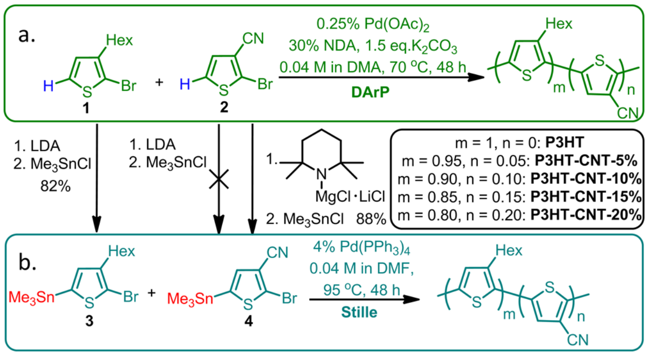

Here we report four P3HT-CNT copolymers synthesized directly from unmetalated and commercially available 2-bromo-3-hexylthiophene (**1**) and 2-bromo-3-cyanothiophene (**2**) (Scheme 1) using the unique DArP reaction conditions previously developed for P3HT[27] and compare their structural and optoelectronic properties, as well as photovoltaic performance with the same polymers synthesized via Stille polymerization.[23] Polymers are identified by the acronym P3HT-CNT-*X*%, where the percentage of CNT unit is indicated. The DArP P3HT-CNT copolymers are found to be remarkably similar to their Stille counterparts in terms of molecular weight and polymer yield, which highlights the feasibility of these unique DArP conditions for the synthesis of P3HT-CNT copolymers. Also their optical, electronic, and photovoltaic properties are found to be close to those of Stille analogues. Importantly, it was found that solar cells based on the DArP copolymers gave FFs comparable to those of Stille analogues. Also, the J_{sc} was significantly enhanced for the DArP polymers, and the V_{oc} values were found to be 30 mV lower than for the Stille polymers. The overall PCE in the case of DArP P3HT-CNT-5% was found to be higher than that of the Stille copolymer (3.64% vs 2.96%). This result is significant since it further demonstrates that DArP is indeed suitable for the synthesis of conjugated polymers for OPV, bringing the advantages of significantly simplified synthesis using inexpensive, stable, and environmentally friendly reagents.

The polymerization conditions for the synthesis of DArP P3HT-CNT copolymers (Scheme 1) include a very low loading of 0.25 mol % of palladium acetate (Pd(OAc)$_2$), 1.5 equiv of potassium carbonate, and 30 mol % of neodecanoic acid (NDA).[28] NDA is thought to be deprotonated by K$_2$CO$_3$ in situ and then act as a bulky carboxylate ligand with high basicity at the palladium center, accelerating the direct arylation reaction rate[29] and, due to bulkiness, limiting the formation of β-defects[30] on the growing polymer chain, as was demonstrated previously for the case of P3HT.[27,31] NDA was introduced by our group as an alternative to the commonly used pivalic acid (PivOH) and has been demonstrated to decrease the amount of defects in the polymer chain and

Table 1. Molecular Weights (PDIs), Electrochemical HOMO Values, Optical Band Gaps, Space-Charge Limited Current (SCLC) Mobilities, and Photovoltaic Performance of DArP and Stille P3HT-CNT[a]

method (yield, %)	polymer	M_n,[b] kg/mol (PDI)	HOMO,[c] eV	E_g,[d] nm/eV	μ,[e] cm^2 V^{-1} s^{-1}	polymer:PC$_{61}$BM ratio[f]	J_{sc},[g] mA cm^{-2}	V_{oc}, V	FF	η, %
DArP (66)	P3HT	16 (2.8)	5.25	645/1.92	1.93×10^{-4}	1:0.9	8.50	0.59	0.54	2.70
Stille (73)	P3HT	18 (2.5)	5.20	646/1.92	2.31×10^{-4}	1:0.9	9.20	0.60	0.57	3.15
DArP (65)	P3HT-CNT-5%	12 (2.9)	5.28	654/1.90	1.10×10^{-4}	1:1.0	9.33	0.69	0.57	3.64
Stille (59)	P3HT-CNT-5%	11 (1.9)	5.30	653/1.90	1.51×10^{-4}	1:1.0	7.02	0.72	0.58	2.96
DArP (63)	P3HT-CNT-10%	11 (2.6)	5.31	659/1.88	7.20×10^{-5}	1:1.3	9.32	0.72	0.49	3.29
Stille (50)	P3HT-CNT-10%	12 (2.4)	5.31	658/1.88	1.03×10^{-4}	1:1.3	8.16	0.75	0.55	3.33
DArP (26)	P3HT-CNT-15%	10 (2.2)	5.35	664/1.87	5.60×10^{-5}	1:1.3	7.87	0.78	0.41	2.52
Stille (25)	P3HT-CNT-15%	10 (2.1)	5.34	653/1.90	8.54×10^{-5}	1:1.3	7.56	0.81	0.55	3.28
DArP (42)	P3HT-CNT-20%	11 (2.8)	5.33	667/1.86	2.90×10^{-5}	-[h]	-	-	-	-
Stille (51)	P3HT-CNT-20%	14 (2.1)	5.31	654/1.87	6.15×10^{-5}	-[h]	-	-	-	-

[a] All values for Stille polymers are taken from ref 23. [b] Determined by GPC with polystyrene as standard and *o*-dichlorobenzene (*o*-DCB) as eluent. [c] Cyclic voltammetry (vs Fc/Fc$^+$) in acetonitrile containing 0.1 M TBAPF$_6$. [d] Calculated from the absorption band edge in thin films, $E_g = 1240/\lambda_{edge}$. [e] Measured for neat polymer films. [f] All devices were spin-coated from *o*-DCB and stored under N$_2$ before aluminum deposition for 30 min. [g] Mismatch corrected. [h] Solar cells were not fabricated for P3HT-CNT-20% due to processing difficulties caused by low polymer solubility.

increase the polymer yield and molecular weight.[27] NDA was used as an inexpensive commercial mixture of structural isomers of tertiary carboxylic acids with the same chemical composition of $C_9H_{19}COOH$. Just like K_2CO_3, NDA is known to be an environmentally benign reagent.[32] DArP is conducted in *N*,*N*-dimethylacetamide (DMA) as a solvent at 70 °C for 48 h. Among the reaction conditions known for DArP, these specific parameters are very attractive since all the reaction components are inexpensive and bench stable and the polymerization does not have to be conducted in a pressurized vessel. What distinguishes these particular DArP conditions from others is the very low loading of palladium acetate, the bulky NDA, and the relatively low reaction temperature, which is below the boiling point of the solvent.

The resulting DArP P3HT-CNT polymers are comparable to their Stille analogues in terms of polymer yield (after Soxhlet extraction) and molecular weights, as shown in Table 1. As the amount of cyanothiophene increases, the polymer yield after purification decreases for both DArP and Stille methods. We speculate that this originates from a decrease in polymer solubility and a decrease in the amount of polymer soluble in chloroform during Soxhlet extraction rather than a decrease in conversion. As such, the polymer solubility steadily decreases with increase of cyanothiophene loading, leading to difficult processing of both DArP and Stille P3HT-CNT-20% at high concentrations.

The composition of the DArP P3HT-CNT copolymers was investigated by ^{1}H NMR, and the complete spectra are shown in the SI (Figures S1−5). In all cases the incorporation ratio of hexylthiophene and cyanothiophene units matched the feed ratio of the corresponding monomers for both DArP and Stille copolymers. The more detailed fragments of the ^{1}H NMR spectra featuring the aromatic region (8.0−6.5 ppm) and a part of the aliphatic region (3.0−2.0 ppm) are illustrated in Figure 1. In the aromatic region, both DArP and Stille copolymers exhibit four main peaks: three smaller peaks of similar intensity (7.37, 7.13, and 7.00 ppm), which likely correspond to predominantly cyanothiophene-containing chain fragments, and one larger peak (at 6.92 ppm), which corresponds to a predominantly hexylthiophene-containing chain fragment.[9] Such an arrangement of peaks in the aromatic regions of ^{1}H NMR spectra of conjugated copolymers has been demonstrated to correspond to a statistical distribution of constituent aromatic units,[33,34] which corroborates the random nature of the P3HT-CNT copolymers. The integral intensity of the three small peaks (7.37, 7.13, and 7.00 ppm) is similar for both DArP and Stille copolymers supporting a random distribution of monomers in both types of polymers. Although very similar to one another, the DArP and Stille copolymers exhibit some differences in the ^{1}H NMR spectra. As such, in the aromatic region for all DArP P3HT-CNT an extra peak at 6.77 ppm is present (marked with an arrow in Figure 1a−c), which is not as pronounced for Stille copolymers, possibly indicating a somewhat different monomer distribution in DArP and Stille copolymers. This peak may also correspond to bromine-terminated hexylthiophene end goups,[35] possibly indicating a somewhat different nature of polymer chain termini between DArP and Stille copolymers. In the case of the Stille reaction, such processes as debromination and aryl group exchange with phosphine ligands are known to cause side reactions,[36] which in the case of Stille polymerization will translate into chain end defects. On the other hand, in the case of DArP the reaction conditions are milder, with lower reaction temperature, significantly lower catalyst loading, and no phosphine ligands, which may explain fewer side reactions that lead to chain end defects. At the same time, in the aliphatic region of all Stille polymers a peak at 2.37 ppm (marked with an arrow in Figure 1a′−c′) can be observed that is not present in any of the DArP polymers. This peak has been postulated to originate from a methyl group on the chain terminus, which comes from an unfavorable transmetalation with trimethylstannylated monomers.[31] Such side reactions have been previously reported for materials obtained via Stille reaction.[37] To summarize, DArP and Stille copolymers are similar in their complete incorporation of both cyanothiophene and hexylthiophene units in the polymer chains. At the same time, there are subtle differences in distribution of the units throughout the polymer chain as well as in the nature of chain termini. Finally, it is important to note that no signals corresponding to β-defects[30,31] are observed in the ^{1}H NMR spectra of DArP copolymers. DArP has previously been demonstrated to produce β-defects (branching points) in conjugated polymers by several research groups,[15,27,30,31,38,39] and for the case of P3HT, a broad peak in ^{1}H NMR at 2.2−2.4 ppm was shown to be diagnostic for the presence of branching defects.[31,39] The absence of any signals in this region for all of the P3HT-based DArP copolymers presented here supports the absence of β-defects, indicating that the DArP conditions used here, which were developed to limit the formation of β-defects in P3HT, translate very well for the case of P3HT-CNT copolymers.[27]

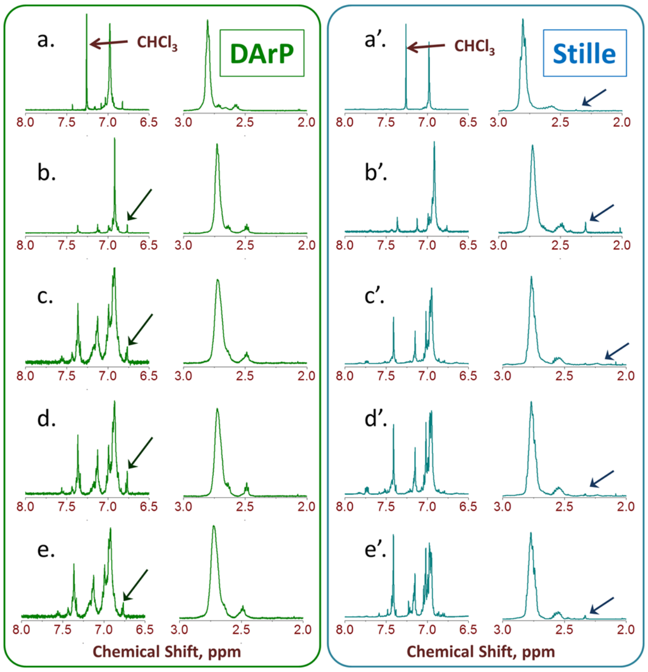

Figure 1. ^{1}H NMR spectra of (a) DArP P3HT; (b) DArP P3HT-CNT-5%; (c) DArP P3HT-CNT-10%; (d) DArP P3HT-CNT-15%; (e) DArP P3HT-CNT-20% and (a′) Stille P3HT; (b′) Stille P3HT-CNT-5%; (c′) Stille P3HT-CNT-10%; (d′) Stille P3HT-CNT-15%; and (e′) Stille P3HT-CNT-20%.

The similarity in the primary chemical structure of DArP and Stille P3HT-CNT copolymers translates into similar absorption profiles as evidenced by the UV−vis absorption spectra of polymer thin films illustrated in Figure 2. The shape of all P3HT-CNT copolymer spectra resembles that of P3HT, exhibiting the absorption onset at ∼650 nm and a vibronic shoulder at ∼600 nm and indicating a semicrystalline nature of

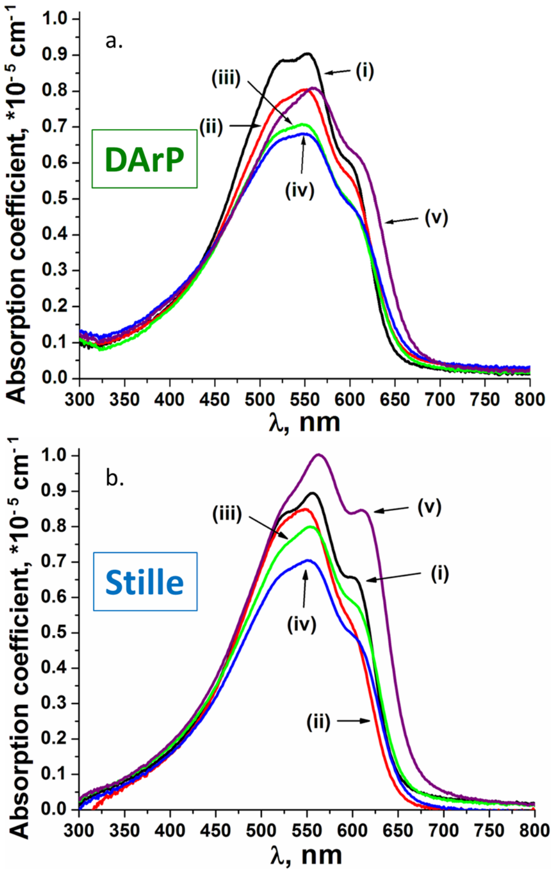

Figure 2. UV–vis spectra of (a) DArP P3HT-CNT and (b) Stille P3HT-CNT thin films, where (i) is P3HT (black line), (ii) is P3HT-CNT-5% (red line), (iii) is P3HT-CNT-10% (green line), (iv) is P3HT-CNT-15% (blue line), and (v) is P3HT-CNT-20% (purple line).

DArP P3HT-CNT copolymers.[40] As the content of cyanothiophene increases from 0% to 15% in both DArP and Stille polymers, the peak absorption coefficient decreases from ~9×10^4 cm^{-1} to ~6×10^4 cm^{-1} (Figure 2 and Table S2, Supporting Information). The vibronic shoulder also becomes less pronounced possibly indicating a decrease in polymer crystallinity. However, when the content of cyanothiophene reaches 20%, the peak absorption coefficient increases to ~8×10^4 cm^{-1} for the case of DArP and to ~1×10^5 cm^{-1} for the case of Stille polymer. This difference may be attributed to slightly lower molecular weight for DArP P3HT-CNT-20% as shown in Table 1. The similarity of DArP and Stille polymers can also be observed in the solution UV–vis spectra shown in Figure S6 (Supporting Information). All the copolymers exhibit a similar absorption profile with the absorption peak shifting to the red part of the spectrum as the content of cyanothiophene increases (Table S2, Supporting Information). The absorption profile is different for DArP P3HT-CNT-20%, which, analogously to Stille P3HT-CNT-20%, demonstrates a vibronic shoulder even in solution indicating a noticeable degree of polymer chain aggregation. At the same time, compared to the Stille polymer, DArP P3HT-CNT-20% has a lower absorptivity in the solution, which possibly originates from somewhat lower molecular weight.

The semicrystalline nature of DArP P3HT-CNT copolymers is also evidenced by the grazing incidence X-ray diffraction (GIXRD) spectra of thin films, where both DArP and Stille copolymers exhibit a pronounced (100) diffraction peak 2θ at ~5.4–5.8 degrees as illustrated in Figure 3. The exact peak position for the DArP polymers is slightly (0.05–0.20 degrees, Table S3, Supporting Information) shifted with respect to the Stille polymers, indicating that the interlamellar d_{100} distance for the DArP polymers is somewhat shorter (by ~0.2–0.5 Å). At the same time the crystallite size for both groups of polymers is very similar (~10–12 nm). Analogously to the UV–vis trend, a decrease in d_{100} peak intensity and a small decrease in the crystallite size can be observed (from 12.69 to 9.51 nm) when the content of cyanothiophene in the polymer backbone increases from 0% to 20%. This may indicate a decrease in crystallinity, likely due to increasing randomness of polymers with higher content of cyanothiophene. Similarly to the Stille P3HT-CNT, DArP polymers display d_{100} decreasing with increasing content of cyanothiophene indicating that the polymer chains pack closer in the (100) direction (Table S3, Supporting Information). As seen previously, DArP P3HT-CNT-20% differs from Stille P3HT-CNT-20%, which exhibits an intensified diffraction peak. As such, DArP and Stille P3HT-CNT are very similar, both having a high degree of semicrystallinity and exhibiting similar trends in the GIXRD spectra when the amount of cyanothiophene is increasing.

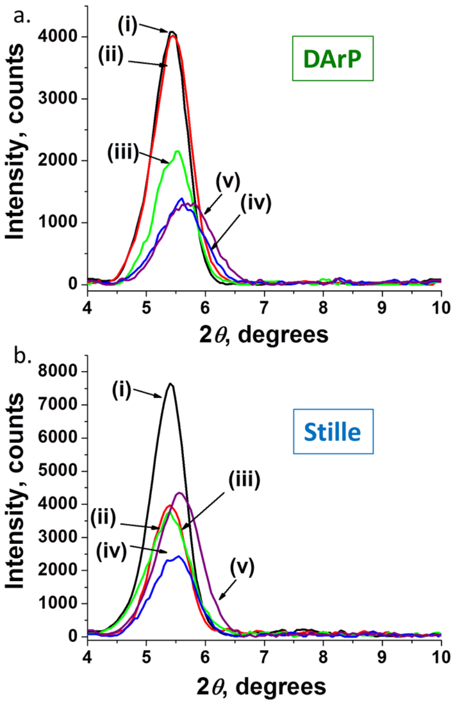

Figure 3. GIXRD spectra of (a) DArP P3HT-CNT and (b) Stille P3HT-CNT thin films, where (i) is P3HT (black line), (ii) is P3HT-CNT-5% (red line), (iii) is P3HT-CNT-10% (green line), (iv) is P3HT-CNT-15% (blue line), and (v) is P3HT-CNT-20% (purple line).

A high degree of semicrystallinity is translated into high SCLC[41] hole mobilities for the neat DArP polymers measured in thin films, as shown in Table 1. The values of hole mobilities for the DArP and Stille pairs of individual polymers are remarkably close, further corroborating the similarity of properties between DArP and Stille copolymers. As is the case with Stille P3HT-CNT, a decrease in hole mobilities can be observed for the DArP group of polymers as the content of cyanothiophene is increased. This could be attributed to a decrease in polymer crystallinity since a similar trend is evidenced by the decrease in intensity of the vibronic shoulder in the UV−vis spectra of thin films as well as a decrease in intensity of the (100) diffraction peak in the GIXRD spectra and the decrease in the crystallite size.

As further evidence of convergence of the electronic properties between DArP and Stille P3HT-CNT copolymers, the oxidation potentials were measured using cyclic voltammetry, and electrochemical HOMO levels were calculated (Table 1).[42] Analogously to Stille P3HT-CNT, DArP copolymers exhibit an increasing oxidation onset and lowering of the HOMO level with the increase in the amount of cyanothiophene; however, in the case of DArP, this dependence is more linear, as illustrated in Figure 4a. Interestingly, when the content of cyanothiophene reaches 20% both DArP and Stille polymers show a sharp decrease in the oxidation onset and, therefore, elevation of the HOMO level. This further illustrates an unusual behavior of P3HT-CNT-20%, probably originating from the strong influence of polymer chain aggregation suggesting that for the practical purpose of photovoltaic application the concentration of cyanothiophene in the polymer backbone should not exceed 15%.

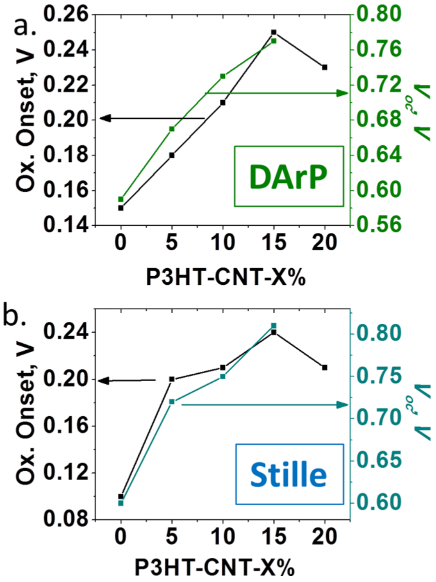

Figure 4. V_{oc} and polymer oxidation onset behavior for (a) DArP P3HT-CNT and (b) Stille P3HT-CNT.

To evaluate the potential for OPV, DArP P3HT-CNT copolymers were utilized as donor materials in organic solar cells with a $PC_{61}BM$ acceptor, and device performance was compared with Stille P3HT-CNT.[23] Organic photovoltaic devices in a conventional device configuration ITO/PEDOT:PSS/polymer:$PC_{61}BM$/Al were fabricated in air. The processing conditions for DArP P3HT-CNT:$PC_{61}BM$ were similar to Stille P3HT-CNT:$PC_{61}BM$ and included solvent annealing after spin-coating from *o*-DCB for 30 min, identical polymer:$PC_{61}BM$ ratios, and in all cases active layer thickness of 75−85 nm. As expected from the cyclic voltammetry (CV) measurements, the V_{oc} of the DArP P3HT-CNT containing solar cells increases with the increase of the CNT content in the polymer backbone, as shown in Table 1 and Figure 4a, and the V_{oc} changes in a similar fashion as the position of the HOMO level (Figure 4a). High FFs were achieved for DArP P3HT, DArP P3HT-CNT-5%, and DArP P3HT-CNT-10%, while in the case of DArP P3HT-CNT-15% lower values were achieved, which can be attributed to the lower hole mobility and possible space-charge build-up.[43,44] High FFs were further supported by transmission electron microscopy (TEM) images which showed the formation of bicontinuous blends with nanometer length scale phase separation (Figure S10, Supporting Information). High V_{oc} and FF obtained in the case of DArP P3HT-CNT:$PC_{61}BM$ are similar to those of Stille P3HT-CNT:$PC_{61}BM$, but at the same time, a few differences are observed. The V_{oc} of DArP P3HT-CNT:$PC_{61}BM$ solar cells is found to be 30 mV lower than that of Stille P3HT-CNT:$PC_{61}BM$ solar cells in all cases. We speculate that this difference originates from the slightly different primary polymer structure, as evidenced by the ^{1}H NMR spectra in Figure 1. Even though the compositions of DArP and Stille P3HT-CNT are identical and lead to similar HOMO and V_{oc} behaviors (Figure 4), small deviations in the monomer distribution and polymer chain termini could affect the V_{oc}.

The largest difference between DArP and Stille P3HT-CNT:$PC_{61}BM$ solar cells was observed in the J_{sc} values. Even though J_{sc} in the case of DArP P3HT was found to be smaller than that of Stille P3HT, significant enhancement of the J_{sc} for DArP P3HT-CNT, especially for DArP P3HT-CNT-5% and DArP P3HT-CNT-10%, was recorded. The difference originates from the increase of the photoresponse in the visible for DArP P3HT-CNT containing polymers, as determined from external quantum efficiency (EQE) studies (Figure S9, Supporting Information). High photocurrent is further supported by the semicrystalline nature of DArP polymers, high hole mobilities, and favorable morphology.[45] The difference between the J_{sc} of DArP and Stille P3HT-CNT:$PC_{61}BM$ solar cells probably, as in the case of the V_{oc}, originates from the difference of CNT monomer unit incorporation in the polymer backbone as well as from the differences in polymer chain termini in the two polymerization procedures.

In conclusion, we have reported a family of four P3HT-CNT copolymers synthesized by DArP and compared their physical, optoelectronic, and photovoltaic properties to the same polymers synthesized by the Stille polymerization. The point of particular importance is that the unique reaction conditions (low 0.25 molar % loading of $Pd(OAc)_2$, bulky NDA, and mild reaction temperature of 70 °C) translate to P3HT-CNT copolymers very well. It was found that DArP copolymers are obtained with yields and molecular weights comparable to those of Stille copolymers. The incorporation ratio of hexylthiophene and cyanothiophene into the polymer chain equals the feed ratio as evidenced by ^{1}H NMR spectra for both DArP and Stille copolymers. Furthermore, the ^{1}H NMR spectra support a statistical distribution of units throughout the polymer chains. At the same time, the monomer incorporation pattern and the nature of the chain termini may be different as evidenced by the subtle differences in the ^{1}H NMR spectra. Importantly, no peaks associated with β-defects were observed in the ^{1}H NMR spectra of DArP copolymers, thus corroborating the suitability of these DArP reaction conditions for the synthesis of P3HT-CNT copolymers. The structural similarity of DArP and Stille copolymers translates into closely matched optoelectronic properties as evidenced by UV−vis and GIXRD spectra, CV traces, and SCLC hole mobilities. In terms of photovoltaic performance, the DArP copolymers demonstrated slightly lower V_{oc} but substantially higher J_{sc} than their Stille counterparts. As a result of high V_{oc}, FF, and enhanced J_{sc}, power conversion efficiencies of DArP P3HT-CNT:$PC_{61}BM$ solar cells were found to be similar to Stille P3HT-CNT:$PC_{61}BM$ solar cells, and in the particular case of P3HT-CNT-5% the DArP copolymer even outperforms its Stille analogue, reaching 3.64% PCE. The obtained results make DArP P3HT-CNT polymers promising wide or intermediate band gap polymers for solar cells, which can be synthesized without the necessity of often difficult monomer stannylation.

■ ASSOCIATED CONTENT

Ⓢ Supporting Information

^{1}H NMR spectra, GIXRD data, UV−vis data, CV traces, TEM images, mobility data, EQE spectra, and J−V data. This material is available free of charge via the Internet at http://pubs.acs.org.

■ AUTHOR INFORMATION

Corresponding Author

*E-mail: barrycth@usc.edu.

Notes

The authors declare no competing financial interest.

■ ACKNOWLEDGMENTS

This material is based upon work supported as part of the Center for Energy Nanoscience, an Energy Frontier Research Center funded by the U.S. Department of Energy, Office of Science, Office of Basic Energy Sciences, under Award DE-SC0001013, specifically for partial support of A.E.R, P.P.K., and B.C.T.

■ REFERENCES

(1) Facchetti, A.; Vaccaro, L.; Marrocchi, A. *Angew. Chem., Int. Ed.* **2012**, *51*, 3520−3523.

(2) Kowalski, S.; Allard, S.; Zilberberg, K.; Riedl, T.; Scherf, U. *Prog. Polym. Sci.* **2013**, *38*, 1805−1814.

(3) Mercier, L. G.; Leclerc, M. *Acc. Chem. Res.* **2013**, *46*, 1597−1605.

(4) Okamoto, K.; Zhang, J.; Housekeeper, J. B.; Marder, S. R.; Luscombe, C. K. *Macromolecules* **2013**, *46*, 8059−8078.

(5) Wang, K.; Wang, M. *Curr. Org. Chem.* **2013**, *17*, 999−1012.

(6) Carsten, B.; He, F.; Son, H. J.; Xu, T.; Yu, L. *Chem. Rev.* **2011**, *111*, 1493−1528.

(7) Sakamoto, J.; Rehahn, M.; Wegner, G.; Schlüter, A. D. *Macromol. Rapid Commun.* **2009**, *30*, 653−687.

(8) Osaka, I.; McCullough, R. D. *Acc. Chem. Res.* **2008**, *41*, 1202−1214.

(9) Chen, T.-A.; Wu, X.; Rieke, R. D. *J. Am. Chem. Soc.* **1995**, *117*, 233−244.

(10) Fuji, K.; Tamba, S.; Shono, K.; Sugie, A.; Mori, A. *J. Am. Chem. Soc.* **2013**, *135*, 12208−12211.

(11) Coffin, R. C.; Peet, J.; Rogers, J.; Bazan, G. C. *Nat. Chem.* **2009**, *1*, 657−661.

(12) Burke, D. J.; Lipomi, D. J. *Energy Environ. Sci.* **2013**, *6*, 2053−2066.

(13) Jo, J.; Pron, A.; Berrouard, P.; Leong, W. L.; Yuen, J. D.; Moon, J. S.; Leclerc, M.; Heeger, A. J. *Adv. Energy Mater.* **2012**, *2*, 1397−1403.

(14) Wang, D. H.; Pron, A.; Leclerc, M.; Heeger, A. J. *Adv. Funct. Mater.* **2013**, *23*, 1297−1304.

(15) Kuwabara, J.; Nohara, Y.; Choi, S. J.; Fujinami, Y.; Lu, W.; Yoshimura, K.; Oguma, J.; Suenobu, K.; Kanbara, T. *Polym. Chem.* **2013**, *4*, 947−953.

(16) Mercier, L. G.; Aïch, B. R.; Najari, A.; Beaupré, S.; Berrouard, P.; Pron, A.; Robitaille, A.; Tao, Y.; Leclerc, M. *Polym. Chem.* **2013**, *4*, 5252−5260.

(17) Kotowski, D.; Luzzati, S.; Bianchi, G.; Calabrese, A.; Pellegrino, A.; Po, R.; Schimperna, G.; Tacca, A. *J. Mater. Chem. A* **2013**, *1*, 10736−10744.

(18) Chang, S.-W.; Waters, H.; Kettle, J.; Kuo, Z.-R.; Li, C.-H.; Yu, C.-Y.; Horie, M. *Macromol. Rapid Commun.* **2012**, *33*, 1927−1932.

(19) Khlyabich, P. P.; Burkhart, B.; Rudenko, A. E.; Thompson, B. C. *Polymer* **2013**, *54*, 5267−5298.

(20) Cosnier, S.; Karyakin, A. *Electropolymerization: Concepts, Materials and Applications*; Wiley-CVH: Weinheim, Germany, 2010.

(21) Shimomura, M.; Kaga, M.; Nakayama, N.; Miyauchi, S. *Synth. Met.* **1995**, *69*, 313−314.

(22) Cheng, Y.-J.; Yang, S.-H.; Hsu, C.-S. *Chem. Rev.* **2009**, *109*, 5868−5923.

(23) Khlyabich, P. P.; Rudenko, A. E.; Thompson, B. C. *J. Polym. Sci., Part A: Polym. Chem.* **2014**, *52*, 1055−1058.

(24) Burkhart, B.; Khlyabich, P. P.; Thompson, B. C. *Macromolecules* **2012**, *45*, 3740−3748.

(25) Krasovskiy, A.; Krasovskaya, V.; Knochel, P. *Angew. Chem., Int. Ed.* **2006**, *45*, 2958−2961.

(26) Greve, D. R.; Apperloo, J. J.; Janssen, R. A. J. *Eur. J. Org. Chem.* **2001**, *2001*, 3437−3443.

(27) Rudenko, A. E.; Wiley, C. A.; Tannaci, J. F.; Thompson, B. C. *J. Polym. Sci., Part A: Polym. Chem.* **2013**, *51*, 2660−2668.

(28) Fefer, M. *J. Am. Oil Chem. Soc.* **1978**, *55*, A342−A348.

(29) Lafrance, M.; Fagnou, K. *J. Am. Chem. Soc.* **2006**, *128*, 16496−16497.

(30) Rudenko, A. E.; Wiley, C. A.; Stone, S. M.; Tannaci, J. F.; Thompson, B. C. *J. Polym. Sci., Part A: Polym. Chem.* **2012**, *50*, 3691−3697.

(31) Rudenko, A. E.; Latif, A. A.; Thompson, B. C. *Nanotechnology* **2014**, *25*, 014005.

(32) Fefer, M.; Rutkowski, A. J. *J. Am. Oil Chem. Soc.* **1968**, *45*, 5−10.

(33) Palermo, E. F.; McNeil, A. J. *Macromolecules* **2012**, *45*, 5948−5955.

(34) Hollinger, J.; Jahnke, A. A.; Coombs, N.; Seferos, D. S. *J. Am. Chem. Soc.* **2010**, *132*, 8546−8547.

(35) Kohn, P.; Huettner, S.; Komber, H.; Senkovskyy, V.; Tkachov, R.; Kiriy, A.; Friend, R. H.; Steiner, U.; Huck, W. T. S.; Sommer, J.-U.; Sommer, M. *J. Am. Chem. Soc.* **2012**, *134*, 4790−4805.

(36) Espinet, P.; Echavarren, A. M. *Angew. Chem., Int. Ed.* **2004**, *43*, 4704−4734.

(37) Leong, W. L.; Welch, G. C.; Kaake, L. G.; Takacs, C. J.; Sun, Y.; Bazan, G. C.; Heeger, A. J. *Chem. Sci.* **2012**, *3*, 2103−2109.

(38) Kowalski, S.; Allard, S.; Scherf, U. *ACS Macro Lett.* **2012**, *1*, 465−468.

(39) Okamoto, K.; Housekeeper, J. B.; Michael, F. E.; Luscombe, C. K. *Polym. Chem.* **2013**, *4*, 3499−3506.

(40) Gurau, M. C.; Delongchamp, D. M.; Vogel, B. M.; Lin, E. K.; Fischer, D. A.; Sambasivan, S.; Richter, L. J. *Langmuir* **2007**, *23*, 834−842.

(41) Kokil, A.; Yang, K.; Kumar, J. *J. Polym. Sci., Part B: Polym. Phys.* **2012**, *50*, 1130−1144.

(42) Cardona, C. M.; Li, W.; Kaifer, A. E.; Stockdale, D.; Bazan, G. C. *Adv. Mater.* **2011**, *23*, 2367−2371.

(43) Qi, B.; Wang, J. *Polym. Chem. Chem. Phys.* **2013**, *15*, 8972−8982.

(44) Kotlarski, J. D.; Moet, D. J. D.; Blom, P. W. M. *J. Polym. Sci., Part B: Polym. Phys.* **2011**, *49*, 708−711.

(45) Brady, M. A.; Su, G. M.; Chabinyc, M. L. *Soft Matter* **2011**, *7*, 11065−11077.